Recent advances in ultrafast optical parametric oscillator frequency combs

Mccracken, Richard A.; Zhang, Zhaowei; Reid, Derryck Telford

Recent advances in ultrafast optical parametric oscillator frequency combs

Richard A. McCracken
Zhaowei Zhang
Derryck T. Reid

SPIE.

Recent advances in ultrafast optical parametric oscillator frequency combs

Richard A. McCracken,* **Zhaowei Zhang,** and **Derryck T. Reid**
Heriot-Watt University, Scottish Universities Physics Alliance, Institute of Photonics and Quantum Sciences, School of Engineering and Physical Sciences, Ultrafast Optics Group, Riccarton, Edinburgh EH14 4AS, United Kingdom

Abstract. We discuss recent advances in the stabilization and application of femtosecond frequency combs based on optical parametric oscillators (OPOs) pumped by femtosecond lasers at 800 and 1060 nm. A method for locking to zero the carrier-envelope-offset of a Ti:sapphire-pumped OPO comb is described. The application of Yb:KYW-laser-pumped dual-combs for mid-infrared spectroscopy is detailed, specifically methane spectroscopy at approximately a 0.7% concentration at 1 atm. © *The Authors. Published by SPIE under a Creative Commons Attribution 3.0 Unported License. Distribution or reproduction of this work in whole or in part requires full attribution of the original publication, including its DOI.* [DOI: 10 .1117/1.OE.53.12.122605]

1 Introduction

Synchronously pumped optical parametric oscillators (OPOs)[1] are a well-established source of ultrashort pulses in the visible to mid-infrared (mid-IR); however, it is only in recent years that their application as a stabilized frequency comb source has been realized and exploited.

Carrier-envelope-phase (CEP) stabilization of OPO pulses was first explored by Kobayashi and Torizuka,[2] who measured the phase relation among subharmonic pulses in a Ti:sapphire-pumped potassium titanyl phosphate (KTP) OPO where the ratio of the idler, signal, and pump frequencies was set to 1:2:3. Stabilization of the relative CEP slip among these subharmonic pulses through OPO cavity length control resulted in an accumulated phase error of only 0.24 rad in the 1-mHz to 1-MHz region.[3] Sun et al.[4] also observed a stable phase relationship between co-resonant signal pulses in a dual-color OPO; subsequent work demonstrated the first fully stabilized frequency comb comprising the pump, signal, and idler pulses by phase locking the Ti:sapphire pump laser and the OPO to a common supercontinuum source.[5,6] Ferreiro et al.[7] demonstrated a simplified method for CEP control of pulses from a femtosecond laser by acquiring a beat between a supercontinuum of the pump pulses and the sum-frequency mixing (SFM) output between the pump and signal pulses, allowing OPO CEP control without f-to-$2f$ self-referencing.

Recent work concerning the operation of a Ti:sapphire-synchronously pumped periodically-poled lithium niobate (PPLN) OPO operating near[8] and at degeneracy[9,10] has shown an operating region where the longitudinal modes of the signal and idler pulses were phase-locked to the pump without active cavity-length stabilization. This work has also been extended to the mid-IR through the use of an Er-fiber-pumped PPLN OPO operating at 3120 nm[11,12] and a Tm-fiber-pumped GaAs OPO operating at 4000 nm in both a degenerate[13] and doubly resonant, nondegenerate state.[14]

In all of the above cases, the absolute phase stability of the OPO modes has not been controlled, since their carrier-envelope-offset (CEO) frequencies simply tracked that of the pump laser, which was not stabilized.

The structure of this article is as follows. In Sec. 2, we review recent trends in ultrafast OPO frequency combs, including advances in coherent pulse synthesis, and mid-IR spectroscopy. Work in the authors' group concerning broadband phase coherence between an OPO and its pump laser is presented in Sec. 3, while our recent progress in asynchronous dual-comb spectroscopy is discussed in Sec. 4. Finally, in Sec. 5, we discuss the outlook for ultrafast OPO frequency combs.

2 Recent Trends in Ultrafast OPO Frequency Combs

2.1 Coherent Pulse Synthesis

Coherent pulse synthesis aims to combine two or more sequences of phase coherent narrowband pulses in order to create a new sequence of identical broadband pulses. In an approach distinct from that based on OPOs, few-cycle and single-cycle pulses have been created[15,16] by using an adiabatically driven Raman resonance[17] to produce monochromatic sidebands that are linearly spaced in frequency and whose phases can be manipulated using a standard Fourier-domain modulator. Coherent synthesis can also be achieved by combining the pulse sequences from two distinct laser oscillators. This was demonstrated by Shelton et al.,[18,19] where the authors synchronized the phases and repetition rates of two mode-locked Ti:sapphire lasers operating at different center wavelengths. Synthesis has also been demonstrated between lasers with different gain media, including Ti:sapphire and Cr:forsterite lasers,[20–22] and a Ti:sapphire and an erbium-doped fiber laser.[23]

CEP stabilized OPOs[24] present a unique vehicle for synthesizing coherent waveforms across wide bandwidths, far exceeding those available from laser gain media.[25] In previous work carried out within the authors' group,

*Address all correspondence to: Richard A. McCracken, E-mail: r.a.mccracken@ hw.ac.uk

a Ti:sapphire-pumped synchronous OPO based on a cascaded-grating MgO:PPLN crystal was used to demonstrate pulse synthesis between the depleted pump pulses and intracavity-doubled-signal pulses from the OPO.[3,26,27] The CEO frequencies of both the pump and doubled signal pulses were locked to the same value. A power spectral density measurement of the CEO frequency stability and an optical cross-correlation measurement between the pump and doubled signal pulses showed that they remained coherent over 1.4 ms with a mutual timing jitter of 30 attoseconds in a 20 millisecond time window.

In Sec. 3, we present recent results demonstrating broadband phase coherence between a pump laser and an OPO and their implications for coherent pulse synthesis are presented.

2.2 Mid-IR Spectroscopy with OPO Frequency Combs

One of the key applications of ultrafast OPO frequency combs is in spectroscopy. Pumped in the near-infrared (NIR) region, a femtosecond OPO can generate broadband emission in the mid-IR, potentially extending throughout the molecular fingerprint region. Such mid-IR combs can replace the black-body radiation sources widely used in a Michelson-interferometer-based Fourier transform infrared (FTIR) spectrometer, enabling fast, sensitive, accurate, free-space, and microspectroscopy-based spectroscopy due to their excellent spatial coherence and high spectral brightness. The first demonstration of OPO spectroscopy was implemented with a free-running OPO comb[28] and later with a fully stabilized OPO comb at the National Institute of Standards and Technology.[29] The benefits of performing spectroscopy using a broadband femtosecond mid-IR OPO are well illustrated by an implementation of methane spectroscopy inside a photonic bandgap fiber.[30–32] These experiments exploited the exceptional spatial coherence and the few 100-cm^{-1} bandwidth of the idler output from a femtosecond OPO to couple 3.3-μm light into the hollow core of a photonic bandgap fiber which had been filled with a mixture of methane and air. The application of frequency-comb techniques to augment methods which exploit this spatial coherence, such as fiber gas sensing, microspectroscopy, and free-space gas sensing, is, therefore, very promising.

Recently, ultrasensitive spectroscopy was demonstrated by the use of intracavity spectroscopy in a broadband OPO comb, pumped by a laser with a free-running CEO frequency.[33] The absence of an intense broadband laser or OPO sources oscillating in the mid-IR meant that until recently, intracavity techniques for mid-IR gas sensing were restricted only to cavity ring-down methods. Intracavity techniques offer a potentially simpler yet highly sensitive route to mid-IR gas sensing.

Another approach to mid-IR spectroscopy is through a dual-comb scheme, in which two asynchronous frequency combs with slightly different mode spacings are heterodyned.[34] When broadband femtosecond pulses are employed in a conventional FTIR spectrometer, the time-domain interferogram encoding the spectral information is constructed from many pairs of pulses which interfere with each other as their relative delay is scanned through a zero path difference. The dual-comb approach can be considered to be analogous to this, but without the need for a mechanically scanning delay line. When two mid-IR combs, identical in all respects except for a small difference in their repetition frequencies (Δf), are combined on a fast photodetector,

an interferogram is produced resulting in a radio-frequency comb of spacing Δf whose Fourier transform provides the spectrum of the mid-IR combs on a frequency scale which is reduced by a factor of $\Delta f / f$ compared to the true optical frequencies. Complete knowledge of the repetition frequencies and CEO frequencies of the mid-IR combs is needed in order to reconstruct the optical spectrum; however, if the CEO frequencies are unknown but stable, then only the center optical frequency is undefined. Determining the relative frequency scale only requires Δf and f, meaning that prior knowledge of the position of a well known spectral feature (e.g., a dominant absorption line) is enough to calibrate the scale. Recently, the use of two asynchronous OPO frequency combs for dual-comb spectroscopy was demonstrated for the first time[35,36] using a scheme in which two repetition-frequency-stabilized lasers pumped a single mid-IR OPO[37] to produce a single dual-comb idler output. In Sec. 4, we present further details relating to this scheme.

3 Broadband Phase Coherence Between an Ultrafast OPO and its Pump Laser

Recently, we reported broadband phase coherence between the pump, signal, idler and related second-harmonic and sum-frequency mixing pulses of an ultrafast OPO.[38] Phase coherence is achieved by locking the CEO frequencies of the pump laser and all the OPO outputs to 0 Hz, while confirmation of coherence takes place through interferometric measurements. This capability is a critical prerequisite for few-cycle coherent pulse synthesis from an OPO.

For coherent pulse synthesis, femtosecond OPOs present a unique opportunity for broadband, low jitter pulse synthesis due to their ability to generate multiple nonlinear mixing frequencies from interactions between the pump (p), signal (s), and idler (i) pulses. An OPO produces fundamental signal and idler frequency combs, as well as new nonlinear frequency-mixing output combs which can be expressed as $f_{NL} = nf_{REP} + qf_{CEO}^p + rf_{CEO}^s$ where n, q, and r are integers. Synthesizing a new pulse sequence from multiple nonlinear mixing outputs requires the parent frequency combs to share a common CEO frequency, which is only generally possible when $f_{CEO}^p = f_{CEO}^s = f_{CEO}^i = 0$. For this reason, it is necessary to lock the CEO frequencies of the pump and either the signal or idler to 0 Hz, with the other automatically locking to 0 Hz as a result of energy conservation in parametric processes.[39]

Locking the CEO frequencies to 0 Hz without using a feed-forward mechanism[40] is achieved by introducing a known frequency shift into one arm of a nonlinear interferometer used for CEO frequency detection. This frequency shifting is performed by an acousto-optic modulator (AOM) driven at f_{SHIFT}, such that the first-order diffracted beam from the AOM carries the additional frequency shift. This diffracted beam is then interfered in a nonlinear interferometer in the usual way[7] and the detected heterodyne beat signal locked to f_{SHIFT}. By detecting and locking the two CEO frequencies from the pump and OPO in this manner, it is possible to achieve broadband zero-offset CEO locking.

The schematic of the zero-offset frequency comb implementation is shown in Fig. 1. Around 85% of the output of a 1.4 W Ti:sapphire laser was used to pump a PPKTP OPO with 20-fs pulses at a repetition frequency of 100 MHz. The OPO was built in a semimonolithic configuration, with the
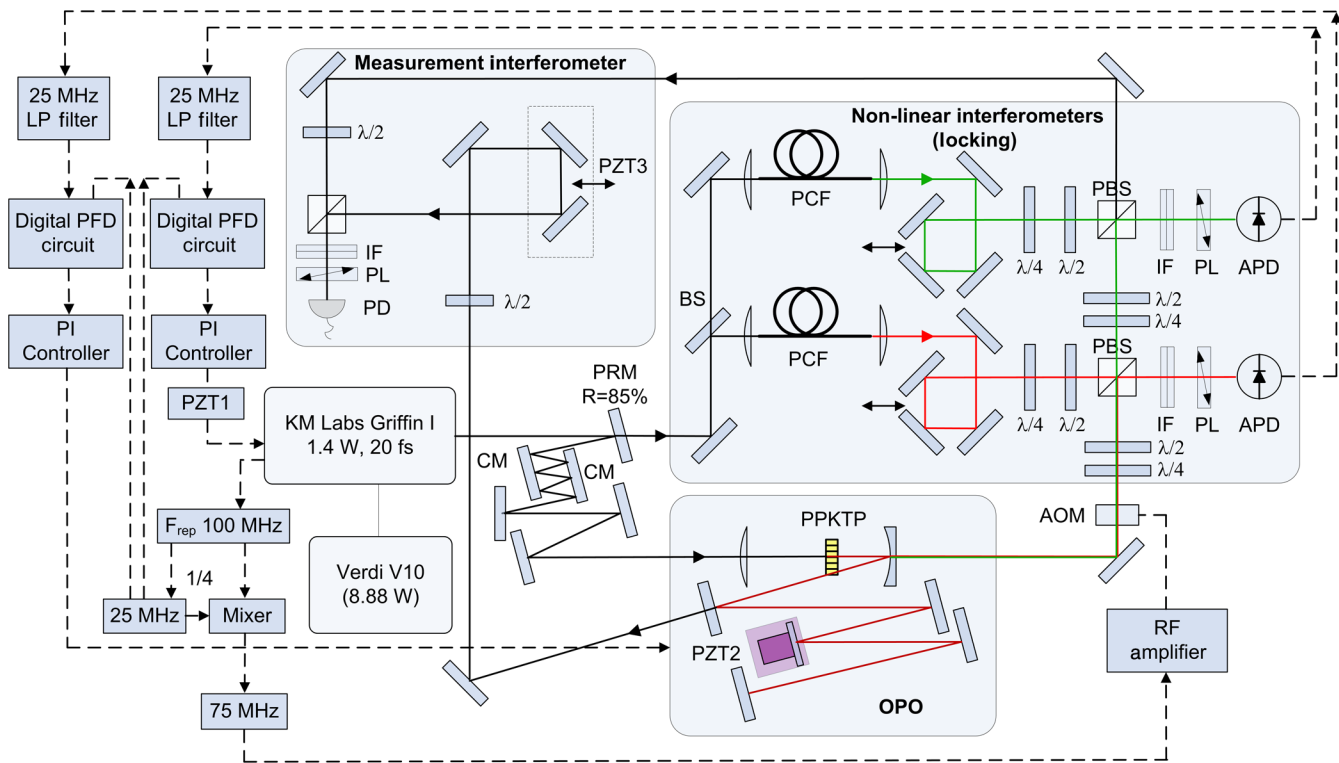
Fig. 1 Optical (solid lines) and electronic (dashed lines) layout of the lock-to-zero optical parametric oscillator (OPO) comb. APD, avalanche photodiode; BS, beam splitter; CM, chirped mirror; IF, interference filter; PBS, polarizing beam splitter; PCF, photonic crystal fiber; PD; silicon photodiode; PI, proportional integral amplifier; and PL, polarizer. See text for other label definitions.

PPKTP crystal coated on one face with an high-reflective (HR)-NIR coating, increasing mechanical stability and minimizing the dispersive broadening of the incident pump pulses. The OPO operated with resonant signal pulses at 1.060 μm, with a range of mW-level visible pulses produced as a result of nonphase-matched nonlinear frequency mixing processes, listed in Table 1. The remaining 15% of the pump power was split and coupled into a pair of photonic crystal fibers (PCFs) to generate two independent pump supercontinua with complementary spectra that overlapped with the $p + i$ and $2s$ visible mixing outputs, as shown in Fig. 2. Using this configuration, an AOM was used to frequency shift the visible outputs of the OPO by $3f_{\mathrm{REP}}/4$ (75 MHz). The pump supercontinuum with the strong green component was interfered with the first-order frequency shifted 0.532 μm light from the OPO in a nonlinear interferometer after a 10-nm bandwidth interference filter. Similarly, the supercontinuum with the strong red component was interfered with frequency shifted 0.642 μm light from the OPO, generated by $p + i$ SFM in the OPO crystal. We refer the reader to Ref. 38 for further details of this configuration.

The electronic signal paths in the CEO-frequency-locking scheme are shown on the left of Fig. 1. The detected CEO frequencies were referenced against a derived $f_{\mathrm{REP}}/4$ signal using a pair of phase-frequency detector (PFD) circuits.[41] The output from the PFD referenced against APD1 was sent to a proportional-integral (PI) amplifier that supplied voltage to a piezoelectric transducer (PZT) attached to a folding mirror in the OPO cavity (Thorlabs Inc., Newton, New Jersey

Table 1 Output wavelengths from the pump and OPO.

Wavelength (μm)	0.400	0.456	0.530	0.642	0.800	1.060	3.260
Origin	$2\omega_p$	$\omega_p + \omega_s$	$2\omega_s$	$\omega_p + \omega_i$	ω_p	ω_s	ω_i
CEO frequency	$2f_{\mathrm{CEO}}^p$	$f_{\mathrm{CEO}}^p + f_{\mathrm{CEO}}^s$	$2f_{\mathrm{CEP}}^s$	$f_{\mathrm{CEO}}^p + f_{\mathrm{CEO}}^i$	f_{CEO}^p	f_{CEO}^s	f_{CEO}^i
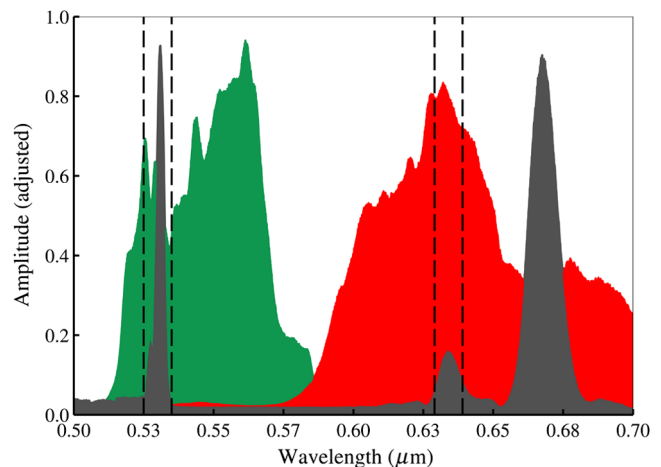
Fig. 2 Spectral overlap regions between the visible OPO outputs (dark area, front) and the two pump supercontinua (large areas, rear left and right). The 0.532 μm SHG signal beam was overlapped with the supercontinuum with a strong green component, while the 0.633 μm SFM pump+idler beam was overlapped with the supercontinuum with a strong red component. The dashed lines indicate the bandpass interference filter regions used to detect a heterodyne beat.

AE0203D04F; 261 kHz unloaded resonance frequency; 4.6 μm maximum displacement, 150 V maximum drive voltage). The corner frequency was 10 kHz, the LF gain limit was 50 dB, and the proportional gain was 5.1. This feedback loop was used to lock the idler CEO frequency. Similarly, the output from the PFD referenced against APD2 was sent to a PI amplifier that drove a PZT in the Ti:sapphire pump laser (>500 kHz unloaded resonance frequency) which was mounted on the cavity end-mirror which received spatially dispersed light from the intracavity dispersion-compensating prism pair. The PI amplifier corner frequency was 10 kHz, the LF gain limit was 50 dB, and the proportional gain was 7.3. This feedback loop was used to lock the pump CEO frequency.

When the system is locked, optical heterodyning at the APD in each nonlinear interferometer produces a frequency at f_{REP} with sidebands at $\pm f_{REP}/4$. Consequently, either beat frequency can be locked to $f_{REP}/4$ or $3f_{REP}/4$, with no electronic means of distinguishing between the two scenarios. This gives a total of four possible locking combinations, only one of which achieves the desired condition of $f_{CEO}^p = f_{CEO}^s = f_{CEO}^i = 0$ Hz. Because of the inherent ambiguity of purely electronic detection, confirming lock-to-zero (and therefore broadband phase coherence) requires optical confirmation through either a spectral or temporal interferometric measurement.

An interferometer was constructed in which residual light from the pump supercontinuum containing a strong 0.530 μm component and a weaker 0.633 μm component was interfered with visible SFM and SHG light exiting OPO folding mirror M2. A temporal interferometry experiment was implemented in which the OPO beam path was modulated using a PZT stage with a frequency of 1.4 Hz and a displacement of 400 μm. The beams were combined and passed through an appropriate interference filter before being detected on a silicon photodiode (Thorlabs DET10A/M). A temporal approach was preferred over a spectral approach due to the poor spatial overlap of the interfering beams and low measurement resolution of the spectrometer.

With the CEO frequencies of the pump and OPO correctly locked, fringes were observed between the pump supercontinuum pulses and the $p + i$ and $2s$ pulses (Fig. 3, blue lines), indicating strong coherence over the 100 ms acquisition time of the interferogram. When either the CEO frequency was unlocked or was locked to a different beat frequency, no fringes were observed, indicating a lack of coherence between the pulses (Fig. 3, red and green lines). In-loop measurements of the cumulative phase noise up to 1 MHz of the pump and OPO CEO frequencies were 0.11 and 0.18 rad over a 1 s observation window. In practice, it was possible to cycle between all four locking combinations through the application of a direct current (DC) offset PZT located in each laser cavity. Approximately 30 V would shift the CEO frequency of either system by $f_{REP}/2$, allowing each source to be locked to the correct locking frequency without realignment of the interferometers.

Observing interference simultaneously at two distinct wavelengths demonstrated that all the CEO frequencies from the pump and OPO were locked to 0 Hz, confirming phase coherence across all the pulses on the optical bench. This coherent bandwidth extends from 0.4 to 3.2 μm and comprises an ensemble of pulses sharing a common zero-offset
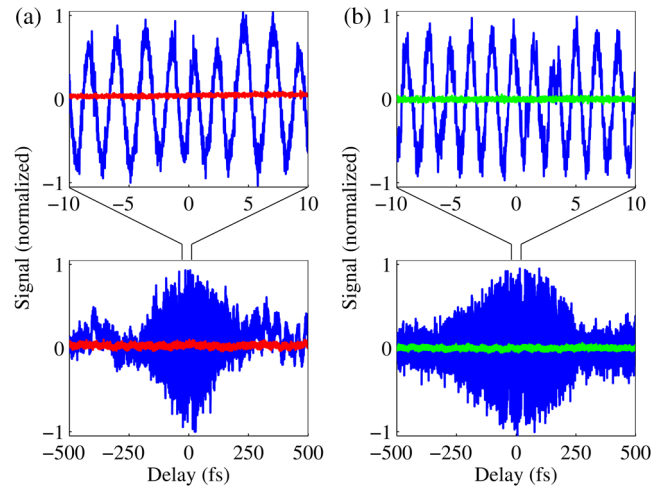

Fig. 3 Interferograms between a pump supercontinuum and (a) $p + i$ and (b) $2s$ leakage light from the OPO. Interference fringes (red, green) were observed when the CEO frequencies of the pump and OPO were locked in the correct configuration. Any other locking configuration resulted in no interference fringes (flat lines).

frequency comb, the broadest zero-offset comb demonstrated to date.

4 Asynchronous Dual-Comb Spectroscopy

Recently, we introduced a dual-comb spectroscopy OPO approach[35] based on combining two repetition-rate-locked Yb:KYW lasers to form a composite pump source for a MgO:PPLN OPO designed to operate simultaneously at two different repetition frequencies.[37] This experiment studied dual-comb spectroscopy of a 1-atm $N_2 : CH_4$ mixture with a low (0.7%) methane concentration in a 20-cm absorption cell. A schematic of the dual-comb system appears in Fig. 4. One of the Yb:KYW lasers served as a master oscillator and was repetition-rate stabilized to 100 MHz, while the other acted as a slave oscillator which could be stabilized at a relative frequency offset to the master oscillator using a phase-locked loop approach.[42] Each Yb:KYW laser produced pulses with an average power of around 100 mW and pulse durations of 150 fs, which were amplified in a separate cladding-pumped polarization-maintaining Yb:fiber amplifiers to up to 3 W average power. The pulses leaving the amplifiers were chirped to durations of 3 ps and −3 dB bandwidths of 10 nm due to a combination of self-phase modulation and linear dispersion. There was no requirement to implement chirped-pulse amplification since modest nonlinear spectral broadening is beneficial to the spectroscopy performance because the OPO design transfers the pump spectral bandwidth into the mid-IR idler output.[43] The pulses from each Yb:fiber amplifier were combined on a 50:50 beam splitter before entering the MgO:PPLN OPO. For operation around 3.3 μm (methane Q branch), the OPO was operated on a grating period of 30.49 μm and the idler light coupled through a dichroic cavity mirror coated with high transmission above 2.5 μm and on a yttrium aluminium garnet (YAG) substrate. This output was directed into the absorption cell and the signal was detected by a thermoelectrically cooled MCZT (HgCdZnTe) photovoltaic detector with a bandwidth of 100 MHz.

Figure 5 illustrates the data acquisition and processing methodology, together with the results from the dual-comb
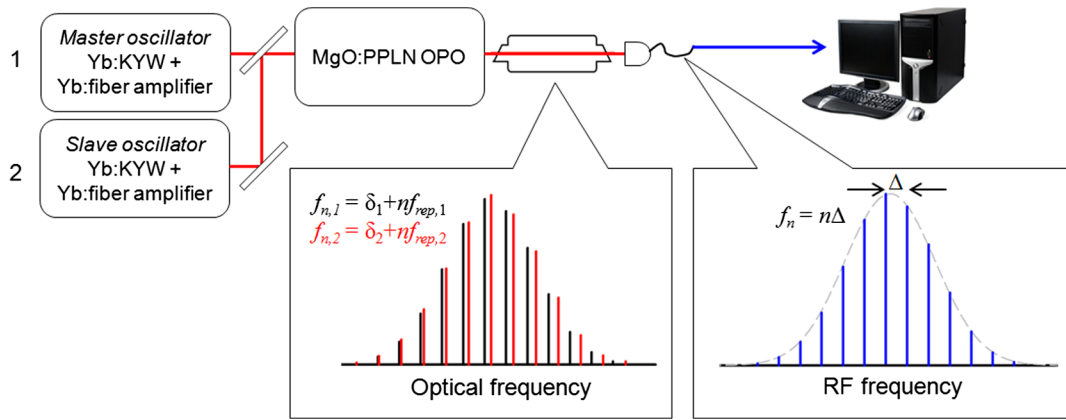
Fig. 4 Mid-IR dual-comb spectroscopy using an OPO. A dual-comb is produced using pulses from two Yb:KYW femtosecond oscillators which have been amplified in separate Yb:fiber amplifiers before being combined in a single MgO:PPLN OPO. The mid-IR dual frequency comb is the idler output of the OPO and comprises two distinct sets of pulses with repetition frequencies $f_{rep,1}$ and $f_{rep,2}$ and carrier-envelope-offset frequencies δ_1 and δ_2. These combs pass through an absorption cell that modulates the intensity of the comb lines before a fast photodetector converts the optical dual-comb into a single radio-frequency comb, spacing Δ, which is digitized using a computer and a fast analog-to-digital acquisition card.
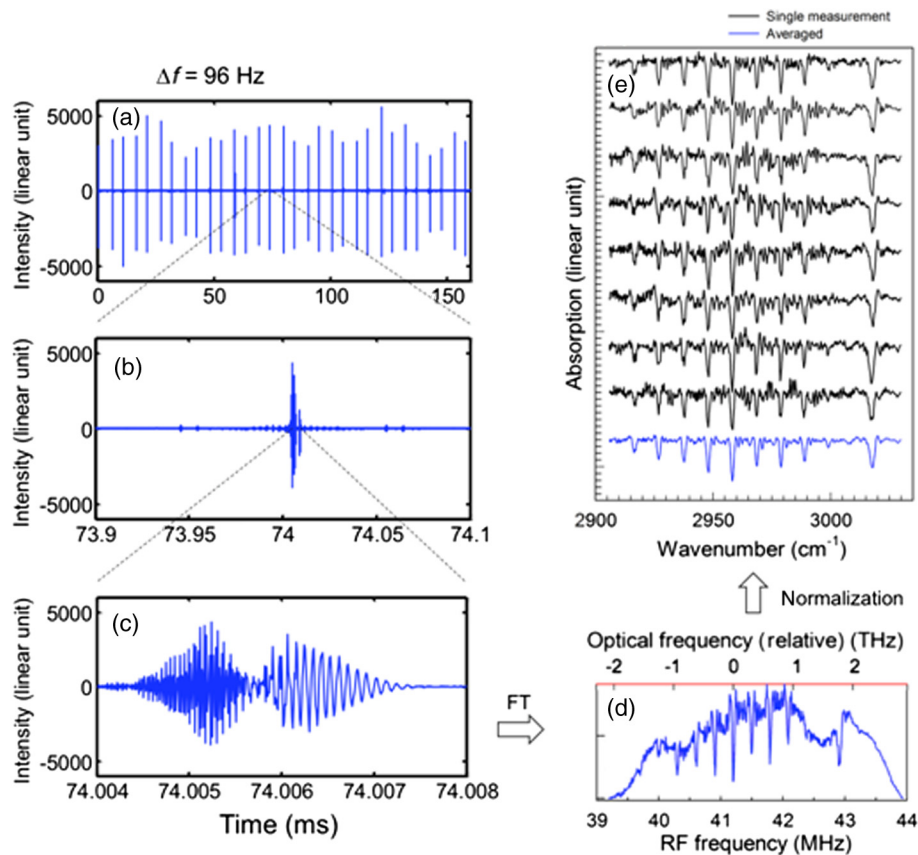
Fig. 5 Data acquisition and analysis procedures for dual-comb OPO spectroscopy of a methane-in-air mixture. The radio-frequency comb comprises time-domain interferograms with a period of Δf, which are sampled at 100 MHz, prior to which they are low-pass filtered at 50 MHz to remove the repetition rate frequency and avoid aliasing. One interferogram is selected, windowed, and Fourier transformed to provide the optical spectrum on a frequency scale with a sampling interval $f/\Delta f$ greater than the frequency interval for the RF comb (the reciprocal of the interferogram time window). An optical spectrum measured without the absorption cell is used to normalize the measurement, allowing the relative absorption to be derived. Multiple interferograms [(e), upper 8 traces] can be used to produce several absorption spectra, which can be averaged to improve the signal-to-noise of the measurement [(e), lower trace].

spectroscopy experiment. In the results presented, the slave oscillator was allowed to be free running at 96 Hz frequency offset from the master oscillator, but this difference was monitored to provide, together with the master oscillator repetition frequency, the calibration factor of $f/\Delta f$ needed to relate the RF- and optical-domain frequencies. The output of the MCZT detector was low-pass filtered to <50 MHz to remove the repetition frequency and then sampled at 100 MS s^{-1} using a 14-bit data acquisition card. The sequence of interferograms acquired in this way over around 150 ms is shown in Fig. 5(a), the period of which provides an exact rendering of the pulse repetition rate difference, Δf. One of the mode-locked Yb:KYW seed lasers was running in double-pulse mode, and this behaviour was transferred to the mid-IR pulse sequence in the OPO. Thus, the interferogram shows two bursts in each period. In processing this signal, we extract one interferogram from the sequence in a time window of around 200 μs [Fig. 5(b)], the detail of which is shown in Fig. 5(c). Next, this individual interferogram is Fourier transformed [Fig. 5(d)] and recalibrated into the optical domain by scaling the frequency axis by a factor of $f/\Delta f$ and centering the data in frequency to align to the Q branch of the methane absorption lines—a step which requires prior knowledge of the absorption features under study (see later discussion). A normalization process is used to remove the envelope of the idler pulses from the data in order to reveal the underlying absorption lines [Fig. 5(e)]. Averaging several absorption spectra obtained in this way allows the noise on the result to be reduced [Fig. 5(e), blue]. The result in Fig. 5(e) is shown in Fig. 6 (blue trace) together with a simulated methane absorption spectrum (red) calculated for a resolution of 0.2 cm^{-1}, a path length of 20 cm, and a concentration of 0.65% methane at 1 atm. There is good agreement in the frequencies of the absorption lines. The correspondence in the intensity is good except above 3005 cm^{-1} where the structure of the Q branch is not fully recovered. The origin of this corruption is the imperfect spectral overlap between the two idler pulse
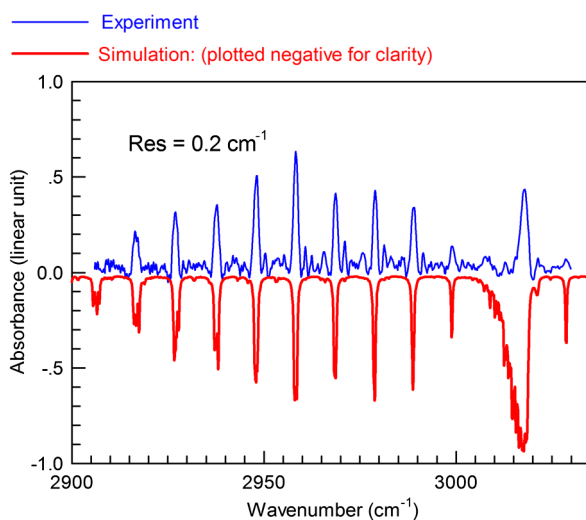
sequences at their long wavelength edges. Using a single OPO to generate both idler pulse sequences has significant advantages, particularly in the fact that these two idler outputs experience excellent spatial overlap. A minor drawback is that the use of two slightly different pump repetition frequencies leads to a small relative detuning of the center wavelengths of the idler spectra, which is most pronounced at their edges, leading to the experimentally observed discrepancy.

The results presented here were obtained without locking the CEO frequencies of either idler pulse sequence. As our results show, CEO locking is not necessary for accurate dual-comb spectroscopy, but allowing the CEO frequencies to be free running presents various advantages and disadvantages. The principal advantage of avoiding CEO stabilization is in terms of simplicity; combs that are only repetition-rate stabilized but are not CEO locked are simpler and potentially more robust to work with. Dual-comb spectroscopy is possible without CEO locking because the measurement is complete within a very short time (sub-ms time scales), during which the f_{CEO} drift is typically small for a well-engineered system. In comparison to other systems, even non-CEO-locked dual-comb spectroscopy offers rapid and high-resolution spectroscopy. The main disadvantages of free-running CEO frequencies are that the full resolution (100 MHz in our system) of the dual-comb measurement is not necessarily available (effectively due to fluctuations in the time base of the measurement) and the central wavelength of the spectrum cannot be extracted. Finally, the absence of an exact knowledge of the comb offsets means there is an ambiguity in the spectral direction, so independent calibration is necessary. Other authors have presented schemes in which the comb offsets and repetition frequencies are recorded but not stabilized during the measurement, allowing the exact comb structure to be reconstructed in real time.[44,45]

5 Conclusions and Future Outlook

Ultrafast OPOs present a unique way of extending the performance of frequency combs into the mid-IR but also into the visible, by exploiting the wide spectral coverage available by combining a tunable NIR/mid-IR OPO comb with second-harmonic and sum-frequency conversion techniques. One area in which tunability into the visible region may be exploited is in the generation of visible combs suitable for the calibration of high-resolution spectrographs. Accessing the full visible range of interest (370 to 800 nm) is difficult to achieve directly from Ti:sapphire combs, but Ti:sapphire-pumped OPO combs can readily address this full region using second-harmonic generation of the pump and signal pulses.

Mid-IR dual-comb spectroscopy using OPOs has the potential to deliver high-speed, high-resolution free-space, and stand-off spectroscopy of remotely located pollutants and chemicals. Dual-comb-based ranging at 1.5 μm for a distance measurement has demonstrated precisions of 5 nm and ambiguity ranges of 30 km.[46] A similar technique is, in principle, possible using mid-IR OPO combs and could be combined with spectroscopy to provide both the range and spectroscopic signature of an object. Dual-comb OPO spectroscopy based on free-running CEO frequencies offers considerable potential in simple, robust, and practical systems. One approach is to use a spectral reference (e.g., a Bragg grating, an etalon, or a molecular absorption line) to provide

Fig. 6 Methane absorption spectrum derived from the dual-comb spectroscopy measurement (top). A simulated methane absorption spectrum (bottom) is presented for simulation parameters of 20-cm path length of 0.65% methane at 1 atmosphere and a spectral resolution of 0.2 cm^{-1}.

a perpetual reference spectrum against which other data can be calibrated. The resolution of such an approach will be limited by high-frequency fluctuations in the CEO frequency, but the disadvantages cited in Sec. 4 can be circumvented to a satisfactory level for many applications by the use of a spectral calibration reference.

References

1. D. C. Edelstein, E. S. Wachman, and C. L. Tang, "Broadly tunable high repetition rate femtosecond optical parametric oscillator," *Appl. Phys. Lett.* **54**, 1728–1730 (1989).
2. Y. Kobayashi and K. Torizuka, "Measurement of the optical phase relation among subharmonic pulses in a femtosecond optical parametric oscillator," *Opt. Lett.* **25**(11), 856–858 (2000).
3. Y. Kobayashi et al., "Optical phase locking among femtosecond subharmonic pulses," *Opt. Lett.* **28**(15), 1377–1379 (2003).
4. J. Sun, B. J. S. Gale, and D. T. Reid, "Dual-color operation of a femtosecond optical parametric oscillator exhibiting stable relative carrier-envelope phase-slip frequencies," *Opt. Lett.* **31**(13), 2021–2023 (2006).
5. J. H. Sun, B. J. S. Gale, and D. T. Reid, "Composite frequency comb spanning 0.4–2.4 μm from a phase-controlled femtosecond Ti:sapphire laser and synchronously pumped optical parametric oscillator," *Opt. Lett.* **32**, 1414–1416 (2007).
6. J. Sun, B. J. S. Gale, and D. T. Reid, "Control of the carrier-envelope phases of a synchronously pumped femtosecond optical parametric oscillator and its applications," *Chin. Sci. Bull.* **53**(5), 642–651 (2008).
7. T. I. Ferreiro, J. Sun, and D. T. Reid, "Locking the carrier-envelope-offset frequency of an optical parametric oscillator without f-2f self-referencing," *Opt. Lett.* **35**(10), 1668–1670 (2010).
8. R. Gebs et al., "1-GHz repetition rate femtosecond OPO with stabilized offset between signal and idler frequency combs," *Opt. Express* **16**(8), 5397–5405 (2008).
9. S. T. Wong et al., "Self-phase-locked degenerate femtosecond optical parametric oscillator," *Opt. Lett.* **33**(16), 1896–1898 (2008).
10. S. T. Wong, K. L. Vodopyanov, and R. L. Byer, "Self-phase-locked divide-by-2 optical paramteric oscillator as a broadband frequency comb source," *J. Opt. Soc. Am. B* **27**(5), 876–882 (2010).
11. N. Leindecker et al., "Broadband degenerate OPO for mid-infrared frequency comb generation," *Opt. Express* **19**(7), 6296–6302 (2011).
12. A. Marandi et al., "Coherence properties of a broadband femtosecond mid-IR optical parametric oscillator operating at degeneracy," *Opt. Express* **20**(7), 7255–7262 (2012).
13. N. Leindecker et al., "Octave-spanning ultrafast OPO with 2.6–6.1 μm instantaneous bandwidth pumped by femtosecond Tm-fiber laser," *Opt. Express* **20**, 7046–7053 (2012).
14. K. F. Lee et al., "Carrier envelope offset frequency of a doubly resonant, nondegenerate, mid-infrared GaAs optical parametric oscillator," *Opt. Lett.* **38**(8), 1191–1193 (2013).
15. A. V. Sokolov and S. E. Harris, "Subfemtosecond pulse generation by rotational molecular modulation," *Phys. Rev. B* **81**, 2894–2897 (1998).
16. M. Shverdin et al., "Generation of a single-cycle optical pulse," *Phys. Rev. Lett.* **94**, 033904 (2005).
17. S. Harris, D. Walker, and D. Yavuz, "Raman technique for single-cycle pulses," *Phys. Rev. A* **65**, 021801 (2002).
18. L.-S. Ma et al., "Sub-10-femtosecond active synchronization of two passively mode-locked Ti:sapphire oscillators," *Phys. Rev. A* **64**, 021802 (2001).
19. R. K. Shelton et al., "Phase-coherent optical pulse synthesis from separate femtosecond lasers," *Science* **293**(5533), 1286–1289 (2001).
20. Z. Wei, Y. Kobayashi, and K. Torizuka, "Relative carrier-envelope phase dynamics between passively synchronized Ti:sapphire and Cr:forsterite lasers," *Opt. Lett.* **27**(23), 2121–2123 (2002).
21. A. Bartels et al., "Broadband phase-coherent optical frequency synthesis with actively linked Ti:sapphire and Cr:forsterite femtosecond lasers," *Opt. Lett.* **29**(4), 403–405 (2004).
22. Y. Kobayashi et al., "Long-term optical phase locking between femtosecond Ti:sapphire and Cr:forsterite lasers," *Opt. Lett.* **30**(18), 2496–2498 (2005).
23. J. A. Cox et al., "Pulse synthesis in the single-cycle regime from independent mode-locked lasers using attosecond-precision feedback," *Opt. Lett.* **37**(17), 3579–3581 (2012).
24. D. T. Reid, B. J. S. Gale, and J. Sun, "Frequency comb generation and carrier-envelope phase control in femtosecond optical parametric oscillators," *Laser Phys.* **18**(2), 87–103 (2008).
25. D. T. Reid et al., "Advances in ultrafast optical parametric oscillators," *Laser Phys. Lett.* **8**(1), 8–15 (2011).
26. B. J. S. Gale, J. H. Sun, and D. T. Reid, "Towards versatile coherent pulse synthesis using femtosecond laser and optical parametric oscillators," *Opt. Express* **16**(3), 1616–1622 (2008).
27. J. Sun and D. T. Reid, "Coherent ultrafast pulse synthesis between an optical parametric oscillator and a laser," *Opt. Lett.* **34**(6), 854–856 (2009).
28. K. A. Tillman et al., "Mid-infrared absorption spectroscopy across a 14.4 THz spectral range using a broadband femtosecond optical parametric oscillator," *Appl. Phys. Lett.* **85**(16), 3366–3368 (2004).
29. F. Adler et al., "Mid-infrared Fourier transform spectroscopy with a broadband frequency comb," *Opt. Express* **18**(21), 21861–21872 (2010).
30. L. W. Kornaszewski et al., "Mid-infrared methane detection in a photonic bandgap fiber using a broadband optical parametric oscillator," *Opt. Express* **15**(18), 11219–11224 (2007).
31. N. Gayraud et al., "Mid-infrared gas sensing using a photonic bandgap fiber," *Appl. Opt.* **47**(9), 1269–1277 (2008).
32. N. Gayraud et al., "Mid-infrared gas sensing using a photonic bandgap fiber as a gas cell," *Spectroscopy* **24**(1), 46 (2009).
33. M. W. Haakestad et al., "Intracavity trace molecular detection with a broadband mid-IR frequency comb source," *J. Opt. Soc. Am. B* **30**, 631–640 (2013).
34. I. Coddington, W. Swann, and N. Newbury, "Coherent multiheterodyne spectroscopy using stabilized optical frequency combs," *Phys. Rev. Lett.* **100**, 013902 (2008).
35. Z. Zhang, T. Gardiner, and D. T. Reid, "Mid-infrared dual-comb spectroscopy with an optical parametric oscillator," *Opt. Lett.* **38**(16), 3148–3150 (2013).
36. Z. Zhang et al., "High-power asynchronous midinfrared optical parametric oscillator frequency combs," *Opt. Lett.* **38**(12), 2077–2079 (2013).
37. Z. Zhang et al., "Asynchronous midinfrared ultrafast optical parametric oscillator for dual-comb spectroscopy," *Opt. Lett.* **37**(2), 187–189 (2012).
38. R. A. McCracken et al., "Broadband phase coherence between an ultrafast laser and an OPO using lock-to-zero CEO stabilization," *Opt. Express* **20**(15), 16269–16274 (2012).
39. J. Sun, B. J. S. Gale, and D. T. Reid, "Testing the parametric energy conservation law in a femtosecond optical parametric oscillator," *Opt. Express* **15**(7), 4378–4384 (2007).
40. S. Koke et al., "Direct frequency comb synthesis with arbitrary offset and shot-noise-limited phase noise," *Nat. Photonics* **4**, 462–465 (2010).
41. M. Prevedelli, T. Freegarde, and T. W. Hänsch, "Phase locking of grating-tuned diode lasers," *Appl. Phys. B* **60**, S241–S248 (1995).
42. Z. Zhang, T. Gardiner, and D. T. Reid, "Asynchronous modelocked Yb:KYW lasers for dual-comb spectroscopy," *Electron. Lett.* **47**(20), 1140–1141 (2011).
43. Z. Zhang et al., "Broadband conversion in an Yb:KYW-pumped ultrafast optical parametric oscillator with a long nonlinear crystal," *Opt. Express* **19**(18), 17127–17132 (2011).
44. J. Roy et al., "Continuous real-time correction and averaging for frequency comb interferometry," *Opt. Express* **20**(20), 21932–21939 (2012).
45. T. Ideguchi et al., "Adaptive real-time dual-comb spectroscopy," *Nat. Commun.* **5**, 3375–3382 (2014).
46. I. Coddington et al., "Rapid and precise absolute distance measurements," *Nat. Photonics* **3**, 351–356 (2009).

Richard A. McCracken received his BSc degree in physics from the University of St. Andrews in 2007 before studying for his MSc degree in photonics and optoelectronic devices in a joint program with Heriot-Watt University, graduating in 2009. He is a research associate at Heriot-Watt University. His current research focuses on high repetition rate optical parametric oscillator frequency combs for astronomical spectroscopy. He then went on to receive a PhD degree from Heriot-Watt University in 2013.

Zhaowei Zhang received his PhD degree from the Optoelectronics Research Center at the University of Southampton. Currently, he is a postdoctoral research associate in the Ultrafast Optics Group at Heriot-Watt University, Edinburgh, UK. His research interests include optical parametric oscillators, fiber lasers, laser frequency combs and their applications for spectroscopy.

Derryck T. Reid received his BA degree from the University of Cambridge in 1991 and a PhD degree from the University of St. Andrews in 1994. During an EPSRC Advanced Research Fellowship from 1997 to 2002, he joined Heriot-Watt University in 2001, where his research addresses the development and applications of femtosecond lasers in microscopy, spectroscopy, and metrology.